BIOCHEMISTRY
including biophysical chemistry & molecular biology

ARTICLE

pubs.acs.org/biochemistry

Identification of Calmodulin and MlcC as Light Chains for *Dictyostelium* Myosin-I Isozymes

Scott W. Crawley,[†] Janine Liburd,[†] Kristopher Shaw, Yoojin Jung, Steven P. Smith, and Graham P. Côté*

Department of Biochemistry, Queen's University, Kingston, Ontario, Canada K7L 3N6

ABSTRACT: *Dictyostelium discoideum* express seven single-headed myosin-I isozymes (MyoA-MyoE and MyoK) that drive motile processes at the cell membrane. The light chains for MyoA and MyoE were identified by expressing Flag-tagged constructs consisting of the motor domain and the two IQ motifs in the neck region in *Dictyostelium*. The MyoA and MyoE constructs both copurified with calmodulin. Isothermal titration calorimetry (ITC) showed that apo-calmodulin bound to peptides corresponding to the MyoA and MyoE IQ motifs with micromolar affinity. In the presence of calcium, calmodulin cross-linked two IQ motif peptides, with one domain binding with nanomolar affinity and the other with micromolar affinity. The IQ motifs were required for the actin-activated MgATPase activity of MyoA but not MyoE; however, neither myosin exhibited calcium-dependent activity. A Flag-tagged construct consisting of the MyoC motor domain and the three IQ motifs in the adjacent neck region bound a novel 8.6 kDa two EF-hand protein named MlcC, for myosin light chain for MyoC. MlcC is most similar to the C-terminal domain of calmodulin but does not bind calcium. ITC studies showed that MlcC binds IQ1 and IQ2 but not IQ3 of MyoC. IQ3 contains a proline residue that may render it nonfunctional. Each long-tailed *Dictyostelium* myosin-I has now been shown to have a unique light chain (MyoB-MlcB, MyoC-MlcC, and MyoD-MlcD), whereas the short-tailed myosins-I, MyoA and MyoE, have the multifunctional calmodulin as a light chain. The diversity in light chain composition is likely to contribute to the distinct cellular functions of each myosin-I isozyme.

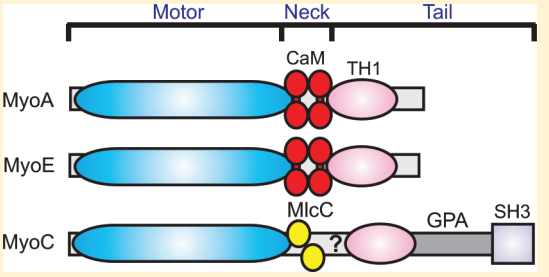

The class I myosins (myosin-I) are a group of widely expressed, single-headed, nonfilament-forming myosins that move actin filaments along cellular membranes.[1,2] Myosin-I consists of a conserved N-terminal motor domain, an α-helical neck region that binds light chains (LCs), and a C-terminal tail. Myosins-I can have a short tail, consisting of a tail homology 1 (TH1) domain that binds acidic phospholipids, or a long tail, consisting of a TH1 domain, a domain rich in glycine, proline, and alanine (GPA) that binds actin filaments, and an SH3 domain.

The biochemical and cellular functions of myosin-I have been extensively studied using the highly motile social amoeba *Dictyostelium*.[3−5] *Dictyostelium* express seven myosin-I isozymes: MyoA, MyoE, and MyoF have short tails; MyoB, MyoC, and MyoD have long tails; and MyoK has no neck or tail but contains a GPA-rich insert in the motor domain. Disruptions of *Dictyostelium* myosin-I genes produce defects in chemotaxis, vesicle transport, cortical tension, phagocytosis, and macropinocytosis.[6−12] Although the loss of a single myosin-I isozyme impairs motile processes, the severity of the phenotype increases when combinations of two or three different myosin-I isozymes are knocked out.[13−15] Myosin-I isozymes therefore have both distinct and redundant functions. The unique functions of individual myosin-I isozymes likely depend on the binding interactions of the tail, the kinetic properties of the motor domain, and the signaling pathways that regulate activity.

Myosin LCs belong to the calmodulin (CaM) superfamily of Ca^{2+}-binding proteins. CaM is 17 kDa in size and consists of two globular domains connected by a flexible linker.[16] Each globular domain is composed of a pair of EF-hand Ca^{2+}-binding motifs. The myosin neck contains α-helical sequences, termed IQ motifs, that bind CaM and CaM-like LCs in the absence of Ca^{2+}.[17] IQ motifs are usually 21−25 residues in length and contain a loosely conserved IQxxxRGxxxR consensus sequence (where x is any amino acid).[17,18] The LCs stiffen the neck region so that it can function as a rigid lever arm to amplify conformational changes in the motor domain.[19] LCs can also act as regulatory elements that control myosin-I motor activity.[20,21]

The LCs for *Dictyostelium* MyoB and MyoD are unique CaM-like proteins. The MyoD LC, MlcD, consists of 147 residues (16.5 kDa) and shares 44% sequence identity with CaM but has lost the ability to bind Ca^{2+}.[22] The MyoB LC, MlcB, is only 73 residues in length (8.3 kDa) and resembles a single lobe of CaM.[23] MlcB has two EF-hand motifs, one of which retains the ability to bind Ca^{2+} with micromolar affinity.

In this report we identify the LCs for three *Dictyostelium* myosin-I isozymes. MyoA and MyoE are shown to associate with CaM in the presence and absence of Ca^{2+}. They represent the first *Dictyostelium* myosins found to employ CaM as a LC. MyoC contains a novel 74-residue LC, termed MlcC. MlcC and MlcB currently provide the only known examples of small single-lobed myosin LCs. In contrast to MlcB, MlcC does not bind Ca^{2+}. The results show that each *Dictyostelium* long-tailed myosin-I (MyoB,

Received: May 9, 2011
Revised: June 13, 2011
Published: June 14, 2011

MyoC, and MyoD) contains a unique, dedicated LC whereas the short-tailed myosins-I (MyoA and MyoE) have CaM as a LC. It is proposed that the diversity in LC composition contributes to the distinct cellular functions exhibited by the *Dictyostelium* myosin-I isozymes.

EXPERIMENTAL PROCEDURES

Plasmid Constructs and Mutagenesis. DNA sequences encoding CaM, MlcC, MyoA, MyoC, and MyoE were obtained by reverse transcription-PCR using poly(A)mRNA extracted from growth-phase *Dictyostelium* AX3 cells with the GeneElute Direct mRNA miniprep kit (Sigma-Aldrich) as the template. First strand cDNA synthesis was performed using Omniscript Reverse Transcriptase (Qiagen) with gene-specific primers. PCR reactions were carried out using the appropriate primers and Expand high fidelity polymerase (Roche Diagnostics). PCR products were initially ligated into the pCR2.1 cloning vector (Invitrogen). The TEDS site residue (Ser-335 for MyoA and Ser-334 for MyoE) was changed to glutamic acid using the QuikChange site-directed mutagenesis kit (Agilent Technologies). For expression in *Dictyostelium*, MyoA, MyoC, and MyoE constructs were cloned into the pTX-FLAG vector which confers G418 resistance and adds an N-terminal FLAG tag.[24] MlcC and CaM were cloned into the pBsrH vector, which confers blasticidin resistance and adds maltose binding protein (MBP) to the N-terminus.[23] For bacterial expression MlcC was cloned into the pET28a vector (Novagen) to add an N-terminal His-tag followed by a thrombin cleavage site. CaM containing a 3′ stop codon was cloned into the NcoI/XhoI sites of the pET28a expression vector (Novagen) which does not add an epitope tag. The fidelity of all constructs were verified by DNA sequencing.

Bacterial Expression of CaM and MlcC. *E. coli* strain BL21-(DE3) containing pET28a vectors encoding CaM or MlcC were grown at 37 °C to an A_{600} of 0.6 in LB medium. Protein expression was then induced by addition of isopropyl β-D-thiogalactopyranoside to a final concentration of 1 mM. After 5 h cells were harvested by centrifugation, resuspended in ice-cold TBS (150 mM NaCl, 50 mM Tris-HCl, pH 7.4) containing 0.2 mg/mL lysozyme and disrupted by sonication. Cell debris was removed by centrifugation at 15000*g* for 1 h. CaM was purified using a heat denaturation step followed by chromatography over a Phenyl Sepharose 6 Fast Flow column (GE Healthcare).[25] MlcC was chromatographed over a 2 mL column of Ni^{2+}-chelating Sepharose beads (GE Healthcare). In some cases on-column cleavage of the His-tag was carried out by incubating the Sepharose beads in 20 mL of 150 mM NaCl, 20 mM Tris-HCl, pH 8.0 containing 100 units of thrombin (Sigma-Aldrich) for 16 h at room temperature. Material eluted from the Ni^{2+}-chelating Sepharose beads was chromatographed over a DEAE column (GE Healthcare) equilibrated in 50 mM NaCl, 20 mM Tris-HCl, pH 7.5. MlcC was eluted stepwise with buffer containing 175, 200, and 300 mM NaCl and then chromatographed over a Hi-Load 16/60 Superdex 75 size exclusion column (GE Healthcare) equilibrated in 150 mM NaCl and 10 mM HEPES, pH 7.4. Fractions containing MlcC were pooled and concentrated using a Millipore Amicon 3 kDa centrifugal device to a final volume of 10 mL and stored at 4 °C. Typically, 7−10 mg of purified MlcC was obtained per liter of cell culture.

Expression and Purification of Recombinant Myosin-I Fragments. pTX-FLAG vectors encoding myosin-I constructs were introduced into *Dictyostelium* AX3 cells by electroporation.[26] Cells were selected for growth in HL5 medium supplemented with penicillin/streptomycin and 20 μg/mL G-418 and/or 10 μg/mL blasticidin.[27] Clonal cell lines were obtained by plating at limiting dilution and were checked for protein expression by immunoblot analysis using monoclonal antibodies against the FLAG tag (F4042, Sigma-Aldrich) or MBP (E8032, New England Biolabs). For purification of myosin-I constructs, cells were grown in 2 L flasks on a gyratory shaker at 200 rpm and 21 °C. Cells were collected by centrifugation and lysed by addition of 0.3% Triton X-100, 50 mM KCl, 2 mM EDTA, 0.2 mM EGTA, 1 mM dithiothreitol, 50 mM Tris-HCl, pH 8.0 containing one Complete Mini protease inhibitor cocktail tablet (Roche Diagnostics) per 50 mL of buffer. The lysate was incubated on ice for 1.5 h to deplete ATP and allow formation of an actin−myosin rigor complex.[28] The pellet was collected by centrifugation at 230000*g* for 1 h and washed several times with 10 mM $MgSO_4$, 30 mM KAc, and 50 mM HEPES, pH 7.3. Recombinant protein was released from the actin filaments by extraction with wash buffer containing 150 mM KCl and 10 mM Mg^{2+}ATP. After centrifugation at 230000*g* for 45 min the supernatant was loaded onto a column containing anti-FLAG M2 agarose beads (Sigma-Aldrich). Recombinant protein was eluted using buffer containing 200 μg/mL of FLAG peptide and was analyzed by SDS-PAGE and by immunoblots using monoclonal antibodies raised against MBP (E8032, New England Biolabs) or *Dictyostelium* CaM (C3545, Sigma-Aldrich).[23]

Mass Spectrometry. Samples of purified MyoA-IQ1,2 or MyoE-IQ1,2 were subjected to SDS-PAGE followed by staining with Coomassie Brilliant Blue. The 17 kDa band was excised, digested with trypsin and chymotrypsin, and analyzed by tandem mass spectrometry (MS/MS) using a Waters Q-TOF Premier mass spectrometer at the Queen's University Protein Function Discovery facility. MS/MS data were used to identify proteins by an MS/MS Ion Search of the Mascot database.[29]

Binding of CaM and MlcC to IQ Motif Peptides. Isothermal titration calorimetry (ITC) experiments were performed using a MicroCal VP calorimeter as described previously.[23] Peptides for ITC analysis were synthesized at the Sheldon Biotechnology Centre, Montreal, Canada. The sequences of the peptides are MyoA-IQ1, residues 718−746; MyoA-IQ2, residues 744−771; MyoE-IQ1, residues 690−719; MyoE-IQ2, residues 718−747; MyoC-IQ1, residues 699−722; MyoC-IQ2, residues 719−740; MyoC-IQ3, residues 737−759. All peptides were acetylated at the N-terminus and amidated at the C-terminus. Peptides, CaM, and MlcC were dialyzed prior to use against 50 mM NaCl, 10 mM HEPES, pH 7.4 and either 2 mM $CaCl_2$ or 2 mM EDTA and 2 mM EGTA. The syringe was loaded with a 350−625 μM solution of the peptide, and 10 μL aliquots were injected into the calorimetric cell containing 25−50 μM CaM or MlcC at 30 °C. The time-dependent differential power signal was integrated to obtain the total heat evolved after each injection of ligand and corrected for the heat of dilution of the ligand alone. Data were analyzed using MicroCal ORIGIN software.

ATPase Assays. ATPase activities were measured by following the release of ^{32}Pi from [γ-^{32}P]ATP.[30] K^+, EDTA ATPase activity assays were performed in 0.5 M KCl, 35 mM EDTA, 1 mM ATP, 25 mM Tris, pH 7.5. Ca^{2+}ATPase activity assays were carried out in 0.5 M KCl, 10 mM $CaCl_2$, 1 mM ATP, 1 mM dithiothreitol, 10 mM TES, pH 7.5. Mg^{2+}ATPase activity assays were carried out in 10 mM $MgCl_2$, 1 mM ATP, 1 mM dithiothreitol, 10 mM TES, pH 7.5 containing either 0.25 mM EGTA or 100 μM $CaCl_2$. Reactions were supplemented with 10 μM

CaM to ensure that the MyoA and MyoE IQ motifs were fully occupied. Rabbit skeletal muscle actin was prepared as described and added at a concentration of 50 μM.[30]

Circular Dichroism Spectroscopy. Far-UV circular dichroism (CD) spectra were obtained using a Chirascan spectrophotometer (Applied Photophysics) and a 0.1 mm path length cuvette containing 20 μM MlcC without the His-tag. MlcC was dialyzed prior to use against 50 mM NaCl, 10 mM HEPES, pH 8.0, and then either 0.2 mM $CaCl_2$, 0.2 mM $MgCl_2$, or 2 mM EDTA was added. Spectra were recorded from 190 to 240 nm at 20 °C and were averaged for six scans. Secondary structure was predicted using the program SpectralWorks (Olis Inc.) with the CONTIN/LL algorithm.[31]

Analytical Ultracentrifugation. Sedimentation velocity experiments were performed using a Beckman Optima XL-1 analytical ultracentrifuge equipped with an AN 60-Ti rotor. MlcC from which the His-tag had been cleaved was dialyzed against 50 mM NaCl, 10 mM HEPES pH 8.0. Dialysis buffer was saved and used in the reference sector for all runs. AUC experiments were run at 20 °C and 50 000 rpm with an MlcC concentration of 60 μM. Cells were scanned for absorbance at 280 nm at intervals of 2 min for a total of 200 scans. Data were analyzed with the SEDFIT program using Lamm equation modeling.[32]

Homology Modeling of MlcC. Comparative modeling of the structure of MlcC bound to MyoC IQ1 was performed using Modeller.[33] A sequence alignment of MlcC with the C-terminal lobe of apo-CaM was used to model the structure of MlcC using the structure of the C-terminal lobe of apo-CaM bound to murine myosin V IQ1 (PDB ID code 2IX7) as a template.[18] Similarly, a sequence alignment of MyoC IQ1 with myosin V IQ1 was used to model the structure of MyoC IQ1 by homology to the structure of myosin V IQ1. One hundred models were generated by Modeller, and the top ranked model was chosen for further analysis. The model was found to have acceptable stereochemistry using PROCHECK[34] and was further validated using the ProSA program which gave a z-score of −5.09, well within the range of z-scores for experimentally determined protein structures of a similar size.[35]

RESULTS

Identification of the MyoA LC. Methods to purify the short-tailed MyoA and MyoE isozymes from *Dictyostelium* have not been developed. The identities of their respective LCs were therefore determined by expressing FLAG-tagged MyoA and MyoE constructs in *Dictyostelium*.

Constructs consisting of the MyoA motor domain (MyoA-M) and the motor domain plus both IQ motifs (MyoA-IQ1,2) were expressed in *Dictyostelium* (Figure 1A). MyoA-M and MyoA-IQ1,2 were isolated from the cytosol in a highly purified state using a Mg^{2+}ATP-dependent actin filament precipitation step followed by affinity purification with anti-FLAG antibody beads (Figure 1A,B). SDS-PAGE analysis of the purified proteins showed that MyoA-IQ1,2, but not MyoA-M, copurified with a 17 kDa protein (Figure 1B). This result identifies the 17 kDa protein as a LC that binds specifically to the IQ motifs in the MyoA neck region. Densitometry of Coomassie blue-stained SDS gels for four different preparations yielded a mean of 1.91 ± 0.56 LCs bound per MyoA-IQ1,2. This is consistent with the presence of two IQ motifs in the neck region of MyoA.

The 17 kDa LC electrophoresed on SDS gels with a mobility similar to that of *Dictyostelium* CaM (Figure 1C). Like CaM, the

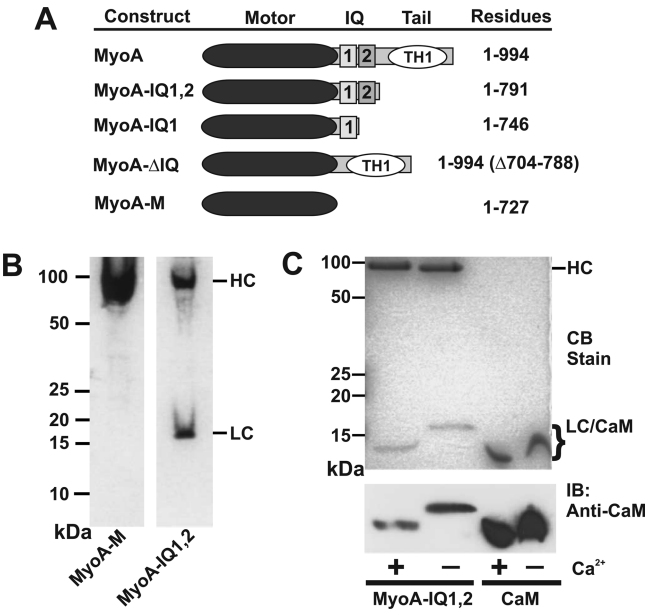

Figure 1. CaM is the LC for *Dictyostelium* MyoA. (A) Domain structure of the MyoA constructs used in this study. (B) The Coomassie blue-stained SDS gel shows Flag-tagged MyoA-M and MyoA-IQ1,2 purified from *Dictyostelium* as described in Experimental Procedures. The location of the MyoA heavy chain (HC) and 17 kDa LC (LC) are indicated. (C) Myo1A-IQ1,2 and *Dictyostelium* CaM were subjected to SDS-PAGE in the absence and presence of 1 mM Ca^{2+}. The upper panel shows a Coomassie blue-stained gel, and the lower panel shows an immunoblot probed with an antibody against *Dictyostelium* CaM. The 17 kDa LC undergoes a Ca^{2+}-dependent mobility shift and reacts with the anti-CaM antibody.

17 kDa LC exhibited an increased electrophoretic mobility in the presence of Ca^{2+} (Figure 1C). The 17 kDa LC also reacted with a monoclonal antibody against *Dictyostelium* CaM (Figure 1C). These results showed that the 17 kDa LC must be either *Dictyostelium* CaM or the closely related calmodulin-like protein B (CalB).[36,37] To confirm its identity, the 17 kDa LC was excised from SDS gels, digested with trypsin and chymotrypsin, and subjected to mass spectrometry analysis. A Mascot Search showed that the top scoring match was *Dictyostelium* CaM (probability-based Mowse score of 229) based on the identification of four separate peptides representing 31% of the sequence.

Identification of the MyoE LC. The MyoE LCs were identified by expressing the MyoE motor domain (MyoE-M) or the motor domain fused to the two IQ motifs in the neck (MyoE-IQ1,2) in *Dictyostelium* with a Flag-tag (Figure 2A). MyoE-M and MyoE-IQ1,2 were expressed as soluble proteins and were purified to homogeneity as described above for the MyoA constructs. SDS-PAGE analysis showed that a 17 kDa LC copurified with MyoE-IQ1,2 but not MyoE-M (Figure 2B). Densitometry of Coomassie blue-stained SDS gels yielded a mean of 1.18 ± 0.25 LCs bound per MyoE-IQ1,2 for four different preparations. The 17 kDa LC shifted its mobility on SDS gels in a Ca^{2+}-dependent manner and reacted with a monoclonal antibody to *Dictyostelium* CaM (Figure 2C). Analysis of the 17 kDa LC by mass spectrometry showed that the top scoring match was *Dictyostelium* CaM (probability-based Mowse score of 92) based on the identification of two separate peptides representing 17% of the sequence. The results show that both MyoA and MyoE have CaM as a LC.

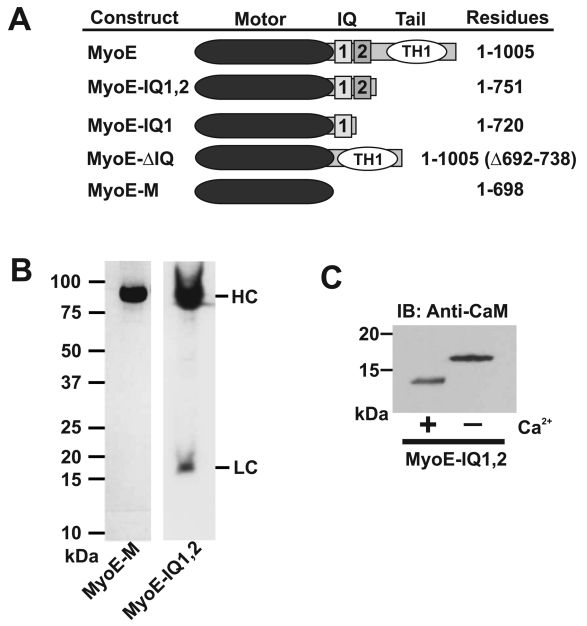

Figure 2. CaM is the LC for *Dictyostelium* MyoE. (A) Domain structure of the MyoE constructs used in this study. (B) The Coomassie blue-stained SDS gel shows Flag-tagged MyoE-M and MyoE-IQ1,2 purified from *Dictyostelium* as described in Experimental Procedures. The locations of the MyoE heavy chain (HC) and 17 kDa LC (LC) are indicated. (C) Immunoblot analysis using an antibody against *Dictyostelium* CaM of Myo1E-IQ1,2 subjected to SDS-PAGE in the presence and absence of 1 mM Ca^{2+}. The 17 kDa LC reacts with the anti-CaM antibody and undergoes a Ca^{2+}-dependent mobility shift.

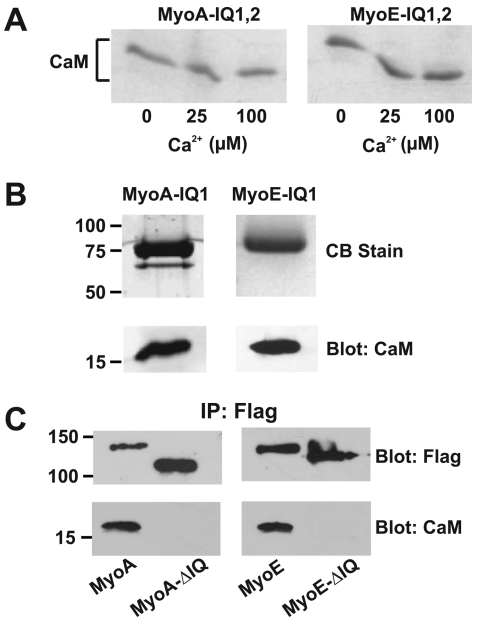

Figure 3. CaM binds to MyoA and MyoE in the presence of Ca^{2+} and the tail. (A) The Coomassie blue-stained SDS gels show MyoA-IQ1,2 and MyoE-IQ1,2 precipitated with actin filaments in the absence of ATP and with the indicated concentration of Ca^{2+}. CaM remains bound to MyoA-IQ1,2 and MyoE-IQ1,2 in the presence of Ca^{2+}. (B) Flag-tagged constructs consisting of the MyoA and MyoE motor domain fused to the first IQ motif (MyoA-IQ1 and MyoE-IQ1) were purified from *Dictyostelium* and analyzed by SDS-PAGE. The upper panels show SDS gels stained with Coomassie blue to visualize the myosin heavy chains. The lower panels show an immunoblot probed with an antibody against *Dictyostelium* CaM. (C) Flag-tagged full-length MyoA and MyoE were immunoprecipitated from *Dictyostelium* cell extracts using an anti-FLAG antibody. Immunoblot analysis was performed using anti-FLAG antibody (upper panels) and antibody against *Dictyostelium* CaM (lower panels). CaM binds to full-length MyoA and MyoE but not MyoA-ΔIQ and MyoE-ΔIQ.

CaM Binds to MyoA and MyoE in the Presence of Ca^{2+} and the Tail. In the experiments described above, MyoA-IQ1,2 and MyoE-IQ1,2 were purified from *Dictyostelium* using buffers containing EDTA and EGTA in order to minimize proteolysis. To examine whether CaM remains bound to MyoA-IQ1,2 and MyoE-IQ1,2 in the presence of Ca^{2+}, actin filament sedimentation assays were carried out. Actin filaments were added to MyoA-IQ1,2 and MyoE-IQ1,2 in the presence or absence of Ca^{2+}, and the resulting complex was collected by centrifugation. Analysis of the complex by SDS-PAGE showed that CaM remains associated with MyoA-IQ1,2 and MyoE-IQ1,2 in the presence of up to 100 μM Ca^{2+} (Figure 3A). Densitometry showed no significant difference in the amount of calmodulin that precipitated with MyoA and MyoE across the three Ca^{2+} conditions tested (data not shown).

CaM was also found to copurify with MyoA and MyoE constructs that contain only the first IQ motif (Figure 3B) and with full-length MyoA and MyoE constructs that contain the tail domain (Figure 3C).

Binding of CaM to IQ Motif Peptides. The sequence of the MyoE IQ1 motif corresponds exactly to the consensus IQ motif sequence, whereas MyoE IQ2 and MyoA IQ1 and IQ2 differ from the consensus sequence at one or more positions (Figure 4). The most divergent sequence is MyoA IQ1, which has Gly in place of the highly conserved Gln at position 2 and a Lys-Met sequence in place of the Arg-Gly sequence at positions 6 and 7. ITC was used to examine the ability of CaM to bind to peptides corresponding to each of the MyoA and MyoE IQ motifs in the presence and absence of Ca^{2+}.

Apo-CaM bound to all four of the MyoA and MyoE IQ motif peptides (Figure 5, left-hand panels). The binding curves could

		1 6 11 IQXXΦRGΦXXR	Net Charge
Consensus			
MyoA IQ1	723	LNDLATKIGSVWKMYKQRKWYL	+4
IQ2	745	RTLAAIKIQRTYRGWLLVRECV	+5
MyoE IQ1	696	MPRIVTLIQKTWRGYRARSKWN	+5
IQ2	718	QRKAAIKIQLFYRSYRYKKWFR	+8
MyoC IQ1	701	WHDMASRIKNAYRNYKAF	+4
IQ2	719	QFECSNRIKNAFRNYKLY	+4
IQ3	737	RQRCAQTIQGYFRAWKQASPFF	+4
MyoB IQ1	768	DFDCTAKIQKAFRNWKAK	+3

Figure 4. Amino acid sequences of the MyoA, MyoB, MyoC, and MyoE IQ motifs. Residues that match the consensus sequence for the IQ motif are highlighted in black. Substitutions of the highly conserved Gln at the +2 position of the IQ motif are shown in gray. Residues in the MyoA and MyoE IQ motifs that correspond to the 1−5−8−14 hydrophobic motif are underlined, and the Pro in the MyoC IQ3 motif is boxed.

be fit well by a single-site model, yielding K_d values that ranged from 0.39 μM for MyoE IQ1 to 2.9 μM for MyoA IQ2 (Table 1). A binding stoichiometry of close to 1.5 peptides per CaM was obtained. This suggests that a fraction of the apo-CaM may be able to bridge two IQ motif peptides.

dx.doi.org/10.1021/bi2007178 |*Biochemistry* 2011, 50, 6579–6588

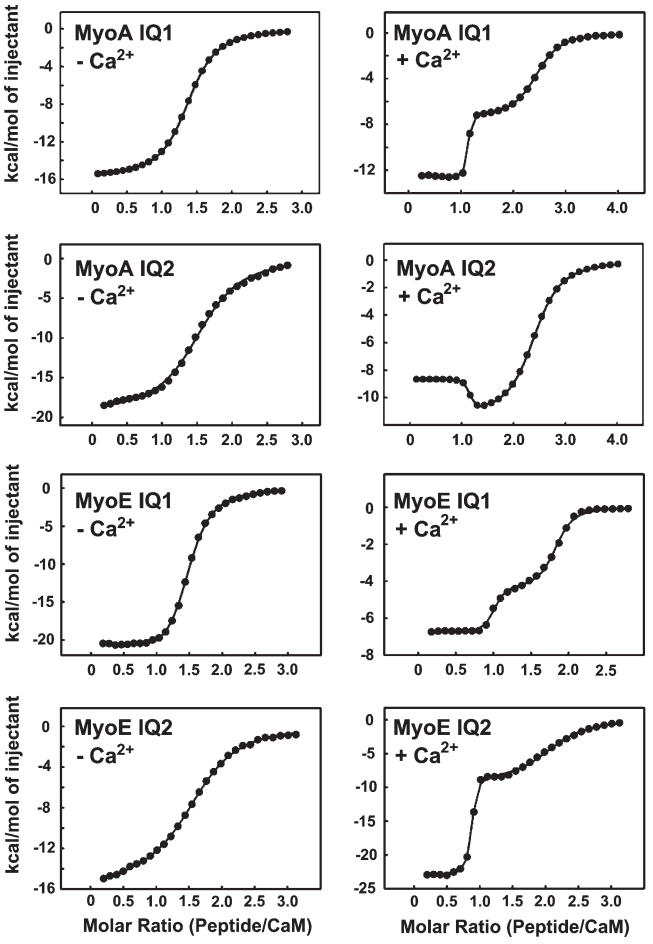

Figure 5. ITC analysis of CaM binding to MyoA and MyoE IQ motif peptides. The ability of CaM to bind peptides corresponding to the MyoA and MyoE IQ motifs was analyzed by ITC in the absence (left panels) or presence (right panels) of Ca^{2+}. The binding isotherms show the total heat per injection (kcal/mol of ligand injected) plotted against the molar ratio of peptide to CaM. Each dot represents an injection of the IQ motif peptide into the ITC cell containing 50 μM CaM. The solid line represents the best fit to the data for a one-site model in the absence of Ca^{2+} and a two-site model out in the presence of Ca^{2+}. The calculated binding parameters are given in Table 1. ITC experiments were performed as described in Experimental Procedures. The results shown are representative plots from three independent experiments.

Table 1. Binding Constants for the Interaction of CaM with IQ Motif Peptides As Determined by ITC[a]

	EGTA		Ca^{2+}	
peptide	N	K_d	N	K_d
MyoA IQ1	1.38 ± 0.04	0.52 ± 0.05 μM	1.07 ± 0.04	0.27 ± 0.06 nM
			1.34 ± 0.01	1.23 ± 0.4 μM
MyoA IQ2	1.54 ± 0.03	2.9 ± 0.15 μM	1.09 ± 0.02	2.40 ± 1.8 nm
			1.29 ± 0.02	1.38 ± 0.1 μM
MyoE IQ1	1.49 ± 0.02	0.39 ± 0.8 μM	0.97 ± 0.01	3.65 ± 1.2 nm
			0.82 ± 0.04	0.62 ± 0.1 μM
MyoE IQ2	1.58 ± 0.05	1.80 ± 0.6 μM	0.83 ± 0.01	4.27 ± 0.8 nm
			1.25 ± 0.02	3.32 ± 0.4 μM

[a] N = stoichiometry of peptide/CaM.

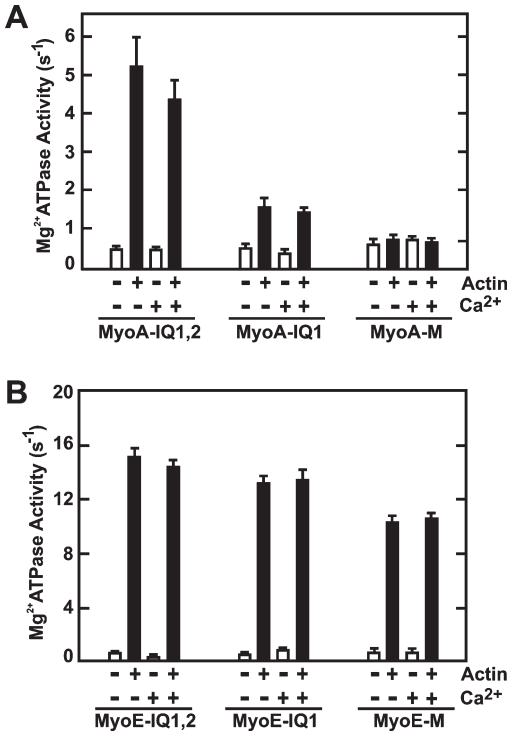

Figure 6. Actin-activated Mg^{2+}-ATPase activities of MyoA and MyoE. Constructs of (A) MyoA and (B) MyoE were assayed for Mg^{2+}-ATPase activity in the presence or absence of actin filaments and the presence or absence of 100 μM Ca^{2+} as described in Experimental Procedures. The results shown represent the mean ± SD for six independent experiments.

In the presence of Ca^{2+}, CaM bound to the IQ motif peptides in a biphasic manner (Figure 5, right-hand panels). The data could be fit well by a two-site model, yielding K_d values of 0.27−4.27 nM for the high affinity interaction and 0.62−3.32 μM for the low affinity interaction (Table 1). The high and low affinity interactions both occurred with a stoichiometry of close to 1, indicating that the N- and C-terminal domains of Ca^{2+}-CaM each bind to a separate IQ motif peptide.

ATPase Activity of MyoA and MyoE. *Dictyostelium* myosins-I exhibit an actin-activated Mg^{2+}ATPase activity only when the TEDS site in the motor domain is phosphorylated.[30,38] For the studies reported here this requirement was eliminated by mutating the TEDS sites of MyoA (Ser-335) and MyoE (Ser-334) to Glu.

MyoA-M exhibited only a minimal actin-activated Mg^{2+}ATPase activity which was increased significantly when IQ1 and IQ2 were fused to the motor domain (Figure 6A). The addition of Ca^{2+} did not alter the actin-activated Mg^{2+}ATPase activity of the MyoA constructs. Thus, the presence of CaM on the IQ motifs, but not its Ca^{2+}-induced conformational change, is required for the activity of MyoA. In contrast, the actin-activated Mg^{2+}ATPase of MyoE-IQ1,2 was only about 50% higher than that of MyoE-M (Figure 6B). Again, no effect of Ca^{2+} on the actin-activated Mg^{2+}ATPase activity of MyoE was observed.

Many myosins display a nonphysiological ATPase activity in 0.5 M KCl that is maximally activated by EDTA.[39] Myo1A-IQ1,2 and Myo1E-IQ1,2 exhibited negligible K^+,EDTA-ATPase activities (<~0.001 s^{-1}). This distinguishes MyoA and MyoE from MyoB, MyoC, and MyoD, which display K^+,EDTA-ATPase activities of between 1 and 10 s^{-1}. Moreover, it suggests an explanation for why purification schemes based on K^+,EDTA-ATPase

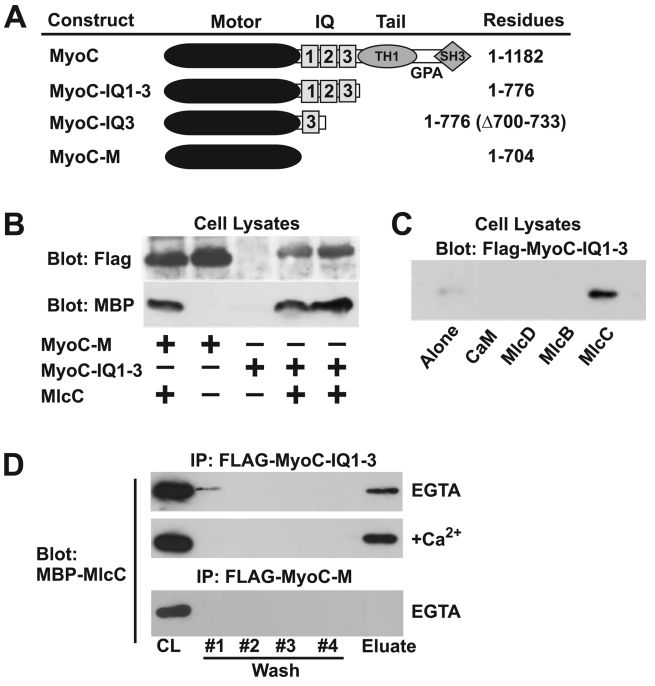

Figure 7. MlcC binds to MyoC. (A) Domain structure of MyoC constructs used in this study. (B) Flag-tagged MyoC-IQ1-3 or MyoC-M were expressed in *Dictyostelium* either with or without MlcC fused to MBP. Total cell lysates were immunobloted using an anti-FLAG and an anti-MBP antibody. The coexpression of MBP-MlcC greatly enhanced the expression of Myo-IQ1-3 by not MyoC-M. (C) Total lysates of *Dictyostelium* cells expressing Flag-tagged MyoC-IQ1-3 along with the indicated MBP fusion protein were probed using an anti-FLAG antibody. Only coexpression of MBP-MlcC enhanced the expression of MyoC-IQ1-3. (D) Flag-tagged MyoC-IQ1-3 or MyoC-M were coexpressed in *Dictyostelium* with MBP-MlcC and immunoprecipitated using anti-FLAG agarose beads. The beads were washed and then eluted using the Flag peptide (Eluate) as described in Experimental Procedures. Samples were immunoblotted using an anti-Flag and anti-MBP antibody. MlcC copurified with MyoC-IQ1-3, but not MyoC-M, in the presence and absence of Ca^{2+}.

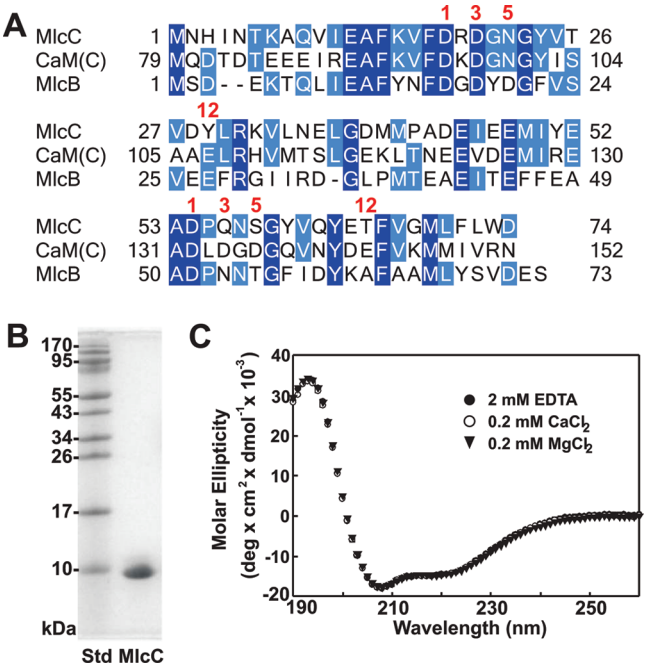

Figure 8. Purification and characterization of MlcC. (A) Alignment of the amino acid sequences of MlcC (dictyBase Gene ID DDB_G0289563; GenBank EAL62662), the C-terminal domain of *Dictyostelium* CaM (CaM(C)) (DDB_G0279407, Genbank EAL67642), and MlcB (DDB_G0290077, Genbank EAL62399). Residues within the two EF-hand Ca^{2+}-binding loops are numbered according to their position. Neither of the MlcC EF-hands contains Glu at position 12. (B) Coomassie blue-stained SDS gel showing recombinant MlcC purified from *E. coli* without the N-terminal His-tag as described in Experimental Procedures. (C) The far-UV CD spectrum of MlcC was measured in the presence of EDTA, Mg^{2+}, or Ca^{2+} as described in Experimental Procedures. Divalent cations did not induce a conformational change in MlcC.

activity have failed to recover MyoA or MyoE.[40] Similarly, neither MyoA nor MyoE displayed detectable Ca^{2+}ATPase activity.

MyoC Binds a Novel Two EF-Hand LC. The neck region of the long-tailed MyoC contains three IQ motifs (Figure 7A). A construct consisting of the MyoC motor domain (MyoC-M) was expressed in *Dictyostelium* cells at a high level, but little or no expression was detected for a construct consisting of the MyoC motor domain fused to the three IQ motifs (MyoC-IQ1-3) (Figure 7B). It was reasoned that the poor expression of MyoC-IQ1-3 might be due to a lack of the appropriate LC, since unliganded IQ motifs can result in aggregated and nonfunctional myosin.[41] The coexpression of CaM, MlcB, or MlcD did not rescue the expression of MyoC-IQ1-3 (Figure 7C). Attention was therefore directed toward other CaM-like proteins that could potentially function as LCs. One of these proteins is MLC-1, a two EF-hand protein of unknown function.[4,23] The studies described below show that MLC-1 is a LC for MyoC and so we will henceforth refer to it as MlcC, for Myosin light chain for MyoC.

The coexpression of MlcC did not affect the expression of MyoC-M but significantly enhanced the expression of MyoC-IQ1-3 (Figure 7B,C). This result suggests that MlcC binds to and stabilizes the MyoC IQ motifs. MlcC co-immunoprecipitated with MyoC-IQ1-3 in the presence and absence of Ca^{2+} but did not co-immunoprecipitate with MyoC-M (Figure 7D). These results show that MlcC binds specifically to the MyoC IQ motifs.

Purification and Characterization of MlcC. MlcC consists of 74 residues and has a molecular mass of 8630 Da. Sequence alignments show that MlcC is most closely related to MlcB, the only other single lobe LC in *Dictyostelium*, and the C-terminal domain of CaM (Figure 8A). To characterize its properties His-tagged MlcC was expressed in *E. coli* and was purified using a procedure that results in proteolytic cleavage of the His-tag (Figure 8B). Subsequent studies showed that the presence or absence of the His-tag had no effect on the properties of MlcC.

To determine its native size, MlcC was analyzed using sedimentation velocity experiments. The sedimentation coefficient distribution showed a single major peak (91% of total) at 1.31 S, which corresponds to a molecular mass of 9.2 kDa, indicating that MlcC is primarily a monomer in solution. CD spectroscopy was used to determine whether MlcC undergoes a conformational change in response to divalent cations. In the absence of Ca^{2+} the far-UV CD spectra of MlcC exhibited a large positive peak of ellipticity at 196 nm and negative peaks of ellipticity near 208 and 222 nm (Figure 8C). Analysis of the spectrum indicates an α-helical content of 57% and a β-sheet content of 10%. The addition of 0.2 mM Ca^{2+} or 0.2 mM Mg^{2+} produced no detectable change in the CD spectrum of MlcC (Figure 8C). Similarly, ITC experiments showed no evidence for a binding

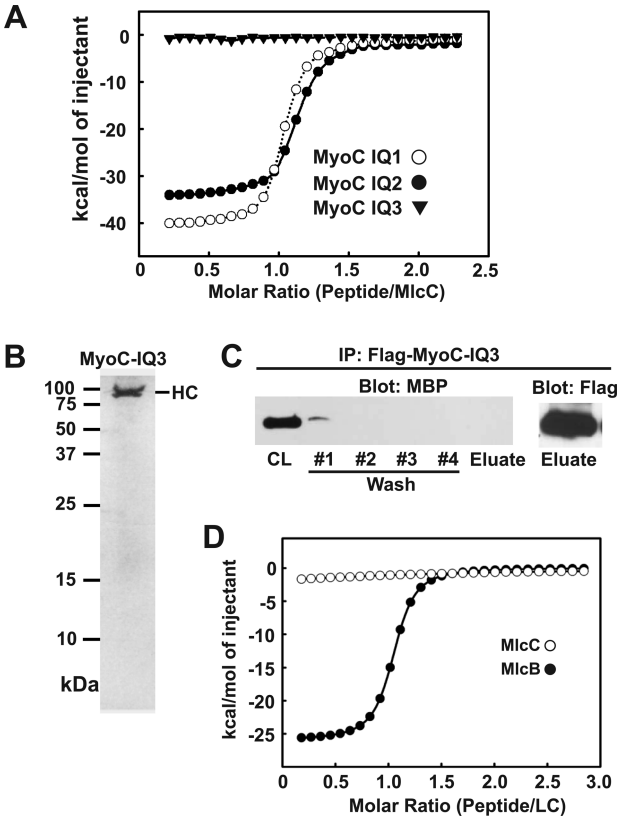

Figure 9. MlcC binds to synthetic peptides corresponding to the MyoC IQ motifs. (A) ITC was used to analyze the binding of MlcC to peptides corresponding to MyoC IQ1, IQ2, and IQ3 motifs as described in Experimental Procedures. The solid line represents the best fit to the data using a one-site model. The calculated binding parameters are given in Table 2. The results shown are representative plots from three independent experiments for each peptide. (B) The silver-stained SDS gel shows Flag-tagged MyoC-IQ3 purified from *Dictyostelium* as described in Experimental Procedures. No LC copurified with MyoC-IQ3. (C) MyoC-IQ3 was coexpressed in *Dictyostelium* with MBP-MlcC and immunoprecipitated using anti-FLAG agarose beads. The beads were washed and then eluted using the Flag peptide (Eluate) as described in Experimental Procedures. Samples were immunoblotted using an anti-Flag and anti-MBP antibody. MlcC did not copurify with MyoC-IQ3. (D) ITC was used to analyze the binding of MlcB and MlcC to a peptide corresponding to the MyoB IQ1 motif as described in Experimental Procedures. The results shown are representative plots from three independent experiments for each protein.

interaction between MlcC and Mg^{2+} or Ca^{2+} ions (data not shown).

MlcC Binds to IQ1 and IQ2 of MyoC. The ability of MlcC to bind to peptides corresponding to IQ1, IQ2, and IQ3 of MyoC was examined using ITC (Figure 4). MlcC bound to the MyoC IQ1 and IQ2 peptides but not to the IQ3 peptide (Figure 9A). The binding curves could be fit well by a one-site model that yielded K_d values of 71 nM for IQ1 and 460 nM for IQ2 (Table 2). No effect of Ca^{2+} on the binding of MlcC to the IQ peptides was observed (data not shown).

The ability of the MyoC IQ3 motif to bind a LC was investigated by expressing a construct in *Dictyostelium* that consisted of the MyoC motor domain and only IQ3 (MyoC-IQ3) (Figure 7A). MyoC-IQ3 was expressed at high levels and could be purified to homogeneity but did not copurify with a LC (Figure 9B). MlcC did not co-immunoprecipitate with MyoC-IQ3, confirming that it binds specifically to the first two IQ motifs of MyoC (Figure 9C).

MlcB and MlcC are the only CaM family proteins in the *Dictyostelium* genome that consist of two EF-hands (Figure 8A).[4,23] MlcB is the LC for MyoB and binds to a peptide corresponding to the MyoB IQ motif with a K_d value of about 500 nM (Figure 9D).[23] MlcC was unable to bind to the MyoB IQ motif, showing that MlcB and MlcC exhibit a different selectivity for IQ motifs (Figure 9D).

Table 2. Binding Constants for the Interaction of MlcC with IQ Motif Peptides As Determined by ITC[a]

peptide	N	K_d
MyoC IQ1	1.06 ± 0.06	71 ± 6 nM
MyoC IQ2	1.09 ± 0.05	0.46 ± 0.04 μM
MyoC IQ3	ND	ND
MyoB IQ	ND	ND

[a] N = stoichiometry of peptide/CaM. ND = not detected.

Table 3. Summary of the LC Composition of *Dictyostelium* Myosin-I Isozymes

isozyme	tail	IQ motifs	IQ motif residues	LC	LC MW (Da)	Ca^{2+} binding
MyoA	short	1	725−746	CaM	17 151	yes
		2	747−768	CaM	17 151	yes
MyoB	long	1	696−717	MlcB	8 296	yes
MyoC	long	1	703−720	MlcC	8 629	no
		2	721−738	MlcC	8 629	no
		3	739−760			
MyoD	long	1	692−713	MlcD	16 519	no
MyoE	short	1	698−719	CaM	17 151	yes
		2	720−741	CaM	17 151	yes
MyoF	short	1	741−762			
		2	781−802			
MyoK	none	none				

DISCUSSION

Dictyostelium Myosin-I LCs. The LCs are integral components of the myosin molecule, and have both structural and regulatory functions. In this study we have identified LCs for three *Dictyostelium* myosin-I isozymes: the short-tailed MyoA and MyoE have CaM as a LC and the long-tailed MyoC has MlcC, a novel two EF-hand protein, as a LC. The LCs for all the *Dictyostelium* myosin-I isozymes, with the exception of MyoF and the third IQ motif of MyoC, are now known (Table 3).[22,23] MyoK has no neck region and is not expected to bind a LC.

Four different CaM family proteins have now been found to function as *Dictyostelium* myosin-I LCs. They can be divided into a pair of four EF-hand proteins, CaM and MlcD, and a pair of two EF-hand proteins, MlcB and MlcC. One member of each pair binds Ca^{2+} with micromolar affinity and undergoes a Ca^{2+}-dependent conformational change (CaM and MlcB), whereas the other member has lost the ability to bind Ca^{2+} (MlcC and MlcD).[22,23]

CaM Binds to the MyoA and MyoE IQ Motifs. MyoA and MyoE are the first *Dictyostelium* myosins to be identified that employ CaM as a LC. CaM also functions as the LC for myosins-I in yeast and mammals. Some myosins-I, including budding yeast Myo5p, fission yeast Myo1p, and vertebrate Myo1a, Myo1b, and

dx.doi.org/10.1021/bi2007178 |*Biochemistry* 2011, 50, 6579–6588

Myo1c, contain one or more IQ motifs that bind CaM weakly in the presence of Ca^{2+}.[42−46] As a result, CaM dissociates from the neck region when Ca^{2+} levels increase and the ability of the myosin-I to move actin filaments is severely inhibited. The dissociation of CaM also induces a conformational change that promotes binding of the Myo5p tail to its targets.[47] Other myosins-I, including mammalian Myo1d and Myo1e, bind CaM in both the presence and absence of Ca^{2+}.[20,48] The studies reported here show that *Dictyostelium* MyoA and MyoE fall into the latter category. Indeed, ITC analysis showed that in the presence of Ca^{2+} the affinity of CaM for the MyoA and MyoE IQ motifs increased ∼1000-fold (Table 1). These results are consistent with previous studies showing that an unidentified short-tailed *Dictyostelium* myosin-I binds to a CaM affinity column in the presence of Ca^{2+}.[25]

IQ motifs that bind Ca^{2+}-CaM with high affinity often contain a 1−5−8−14 pattern of hydrophobic residues characteristic of canonical Ca^{2+}-dependent CaM-binding motifs.[17] This pattern of hydrophobic residues is conserved in all four of the MyoA and MyoE IQ motifs (Figure 4). The MyoA and MyoE IQ motifs also exhibit an overall positive charge, another feature typical of Ca^{2+}-CaM target sequences. The ITC experiments clearly show that in the presence of Ca^{2+} each CaM molecule binds to two IQ motif peptides. This suggest that Ca^{2+}-CaM bridges two IQ motif peptides, with one lobe binding to a peptide with a nanomolar affinity and the other lobe binding to a second peptide with a micromolar affinity. Studies with the individual lobes of CaM show that the C-terminal lobe is most likely to be responsible for the high affinity interaction with the IQ motif peptide.[49,50] Ca^{2+}-CaM has previously been shown to bind peptides based on the myosin V IQ3 and IQ4 motifs with a 2:1 stoichiometry.[49,50] The physiological significance of the 2:1 binding mode is not clear but raises the possibility that Ca^{2+}-CaM can cross-link two myosin-I molecules via their IQ motifs.

The fusion of the IQ motifs to the motor domain significantly enhanced the actin-activated Mg^{2+}-ATPase activity of MyoA but had only a small effect on the activity of MyoE. Although this result provides evidence that the neck region can influence motor activity, no effect of Ca^{2+} on the actin-activated Mg^{2+}-ATPase activity of MyoA or MyoE was observed. This is in contrast to mammalian Myo1d and Myo1e, where a Ca^{2+}-induced conformational rearrangement of CaM on the IQ motifs produces a 2−3-fold decrease in actin-activated Mg^{2+}-ATPase activity.[20,48] Further studies will be required to determine whether Ca^{2+} binding to CaM regulates the conformation of MyoA and MyoE or the properties of the motor domain. Studies on a MyoE motor domain attached to a synthetic lever arm consisting of α-actinin repeats show that it switches its properties from those typical of a fast moving motor toward one designed for tension generation depending on the Mg^{2+} concentration.[8] It will be interesting to determine whether CaM within a native neck region renders the motile and tension generating properties of MyoA or MyoE sensitive to Ca^{2+}.

MlcC Binds to IQ1 and IQ2 of MyoC. Several lines of evidence indicate that MlcC, a novel protein consisting of two EF-hands, is a LC for the first two IQ motifs of MyoC. First, the coexpression of MlcC significantly elevated the expression level of a MyoC motor-neck domain construct (MyoC-IQ1-3) showing that it is able to stabilize the IQ motif sequences. Second, MlcC co-immunoprecipitated with MyoC-IQ1-3, but not MyoC-M or MyoC-IQ3, illustrating that it interacts specifically with IQ1 and IQ2. Third, recombinant MlcC bound tightly to peptides corresponding to MyoC IQ1 and IQ2 but not IQ3. MyoC IQ3 contains a Pro residue at position 13 (Figure 4). Pro residues, which break α-helices, are normally excluded from IQ motifs, suggesting that IQ3 may not be a functional binding site for LCs.[17]

The lack of expression of MyoC-IQ1-3 in *Dictyostelium* contrasts with the high level of expression of MyoA-IQ1,2 and MyoE-IQ1,2. It can be postulated that this difference in expression levels reflects the relative intracellular free concentrations of MlcC and CaM. In mammalian cells at resting levels of Ca^{2+} the free CaM concentration is estimated to be ∼10 μM.[51] A comparable concentration of apo-CaM in *Dictyostelium* would be sufficient to saturate the MyoA and MyoE IQ motifs and allow for expression of soluble protein. MlcC, as a specialized LC, is likely to be present at much lower levels than CaM. Overexpression of MlcC is therefore required for sufficient protein to be present to occupy the IQ motifs and prevent aggregation and degradation of MyoC-IQ1-3.

MlcC shares a much higher degree of sequence identity with the CaM C-terminal domain (43%) than with the N-terminal domain (28%). In the *Dictyostelium* genome the C-terminal domain of CaM (residues 78−152) is encoded by a separate exon.[52] Duplication of this exon would result in an independently folding domain with Met79 as the translation initiation site, which corresponds exactly to the start site of MlcC (Figure 8A). It therefore seems plausible that MlcC arose via duplication of the C-terminal CaM exon. MlcB, on the other hand, exhibits the same amount of sequence identity (∼29%) with both the N- and C-terminal domains of CaM.[23]

Both of the EF-hand motifs of MlcC contain substitutions that would be expected to severely impair Ca^{2+} binding (Figure 8A). Canonical EF-hands contain a 12-residue long Ca^{2+}-binding loop, in which residues at positions 1, 3, 5, and 12 provide side chain oxygen ligands for the Ca^{2+} ion.[53] In functional EF-hands position 12 is invariably filled by a Glu or Asp residue, which provides a bidentate oxygen ligand for Ca^{2+}. In the first EF-hand of MlcC position 12 is filled by a Tyr, and in the second EF-hand it is filled by a Thr (Figure 8A). The absence of an acidic residue at position 12 in the two EF-hands is likely to account for the inability of MlcC to bind Ca^{2+}.

Model for Binding of MlcC to the MyoC IQ Motifs. The first two IQ motifs of MyoC are unusually short, with only 18 residues separating IQ1 from IQ2 and IQ2 from IQ3 (Figure 4). This compares to the IQ motifs in MyoA and MyoE, which are 22 residues in length, and murine myosin V, which are 23 or 25 residues in length (Figure 4).[18] The structure of apo-CaM bound in tandem to the first two IQ motifs of myosin V shows that when the IQ motifs are 23 residues in length, the N- and C-terminal lobes of the two adjacent CaM molecules interact.[18] The MyoC IQ1 and IQ2 motifs are therefore too short to be able to bind both the N- and C-terminal lobes of a conventional LC without considerable steric hindrance.

Homology modeling of the structure of MlcC in a complex with MyoC IQ1was carried out using the program Modeller with the structure of the C-terminal lobe of apo-CaM bound to IQ1 of myosin V as a template (Figure 10). The top-ranked model predicts that MlcC can adopt a structure virtually identical to that of the C-terminal lobe of apo-CaM when bound to the IQ motif. Hydrophobic interactions between the CaM C-terminal lobe and residues in the IQ1 motif of myosin V (Leu766, Ala769, Cys770, Ile773, Ile777, and Trp780) are largely conserved in the model between MlcC and equivalent hydrophobic residues in the MyoC IQ1 motif (Trp701, Met704, Ala705, Ile708, Tyr712, and Tyr715).

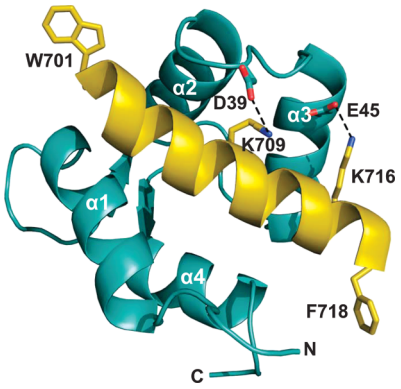

Figure 10. Model of MlcC bound to the MyoC IQ1 motif. The model of MlcC (green) bound to MyoC IQI (yellow) was generated by the program Modeller using the structure of the C-terminal lobe of apo-CaM bound to murine myosin V IQ1 (PDB ID code 2IX7) as a template. Residues at the beginning and end of the IQ motif and those involved in salt bridge interactions are shown in stick representation. The model shown had the lowest modeler objective function out of 100 models generated.

MyoC IQ1 and IQ2 are unusual in that they have a Lys at position 2 instead of the highly conserved Gln that is normally present at this position (Figure 4). In the model the Lys at position 2 (Lys709 in MyoC IQ1) forms a salt bridge with Asp39 which is located in the loop connecting the two EF-hands of MlcC (Figure 10). A comparison of the sequences of IQ1 and IQ2 of MyoC with the IQ motif of MyoB, to which MlcC does not bind, shows that the Lys at position 2 is one of the few significant differences between these sequences (Figure 4). The model indicates that a second salt bridge can be formed between Lys716 at position 9 in the IQ motif and Glu45 in MlcC (Figure 10). However, this interaction cannot account for the specific binding of MlcC since many other *Dictyostelium* myosin-I IQ motifs, including the MyoB IQ motif, have a Lys or Arg at this position (Figure 4). The analysis suggests that the short length of the MyoC IQ1 and IQ2 motifs combined with the presence of Lys at the +2 position may contribute to the specificity of binding of MlcC.

The studies reported here show that CaM is the LC for two short-tailed Dictyostelium myosin-I isozymes, MyoA and MyoE. In contrast, each of the long-tailed Dictyostelium myosin-I isozymes, MyoB, MyoC, and MyoD, are now known to bind a unique LC (MlcB, MlcC, and MlcD, respectively). The diversity in LC composition is likely to contribute to the specialized functions of the individual myosin-I isozymes, both in terms of their ability to respond to changes in intracellular Ca^{2+} levels and to generate movement or force.

AUTHOR INFORMATION

Corresponding Author

*Phone: (613) 533-2998. Fax: (613) 533-2497. E-mail: coteg@queensu.ca.

Author Contributions

†These authors contributed equally to this work.

Funding Sources

This research was funded by an NSERC Group Discovery Grant to G.P.C. and S.P.S. and a Canadian Institutes of Health Research grant (#MOP8603) to G.P.C.

ACKNOWLEDGMENT

We thank David McLeod and Kim Munro of the Protein Function Discovery Facility, Queen's University, for help carrying out mass spectrometry experiments and CD and ITC studies.

ABBREVIATIONS

LC, light chain; MBP, maltose binding protein; CaM, calmodulin; MlcC, myosin light chain of MyoC; MlcB, myosin light chain of MyoB; MlcD, myosin light chain of MyoD; ITC, isothermal titration calorimetry.

REFERENCES

(1) Kim, S. V., and Flavell, R. A. (2008) Myosin I: from yeast to human. *Cell. Mol. Life Sci. 65*, 2128–2137.

(2) Krendel, M., and Mooseker, M. S. (2005) Myosins: tails (and heads) of functional diversity. *Physiology 20* (239−51), 239–251.

(3) De La Roche, M. A., and Côté, G. P. (2001) Regulation of *Dictyostelium* myosin I and II. *Biochim. Biophys. Acta 1525*, 245–261.

(4) Kollmar, M. (2006) Thirteen is enough: the myosins of *Dictyostelium discoideum* and their light chains. *BMC Genomics 7*, 183.

(5) Soldati, T., Geissler, H., and Schwarz, E. C. (1999) How many is enough? Exploring the myosin repertoire in the model eukaryote *Dictyostelium discoideum*. *Cell Biochem. Biophys. 30*, 389–411.

(6) Dai, J., Ting-Beall, H. P., Hochmuth, R. M., Sheetz, M. P., and Titus, M. A. (1999) Myosin I contributes to the generation of resting cortical tension. *Biophys. J. 77*, 1168–1176.

(7) Wessels, D., Murray, J., Jung, G., Hammer, J. A., III, and Soll, D. R. (1991) Myosin IB null mutants of Dictyostelium exhibit abnormalities in motility. *Cell Motil. Cytoskeleton 20*, 301–315.

(8) Durrwang, U., Fujita-Becker, S., Erent, M., Kull, F. J., Tsiavaliaris, G., Geeves, M. A., and Manstein, D. J. (2006) Dictyostelium myosin-IE is a fast molecular motor involved in phagocytosis. *J. Cell Sci. 119*, 550–558.

(9) Schwarz, E. C., Neuhaus, E. M., Kistler, C., Henkel, A. W., and Soldati, T. (2000) *Dictyostelium* myosin IK is involved in the maintenance of cortical tension and affects motility and phagocytosis. *J. Cell Sci. 113*, 621–633.

(10) Wessels, D., Titus, M. A., and Soll, D. R. (1996) A *Dictyostelium* myosin I plays a crucial role in regulating the frequency of pseudopods formed on the substratum. *Cell Motil. Cytoskeleton 33*, 64–79.

(11) Titus, M. A., Wessels, D., Spudich, J. A., and Soll, D. (1993) The unconventional myosin encoded by the *myo*A gene plays a role in *Dictyostelium* motility. *Mol. Biol. Cell 4*, 233–246.

(12) Neuhaus, E. M., and Soldati, T. (2000) A myosin I is involved in membrane recycling from early endosomes. *J. Cell Biol. 150*, 1013–1026.

(13) Jung, G., Wu, X. F., and Hammer, J. A., III (1996) Dictyostelium mutants lacking multiple classic myosin I isoforms reveal combinations of shared and distinct functions. *J. Cell Biol. 133*, 305–323.

(14) Novak, K. D., Peterson, M. D., Reedy, M. C., and Titus, M. A. (1995) *Dictyostelium* myosin I double mutants exhibit conditional defects in pinocytosis. *J. Cell Biol. 131*, 1205–1221.

(15) Falk, D. L., Wessels, D., Jenkins, L., Pham, T., Kuhl, S., Titus, M. A., and Soll, D. R. (2003) Shared, unique and redundant functions of three members of the class I myosins (MyoA, MyoB and MyoF) in motility and chemotaxis in Dictyostelium. *J. Cell Sci. 116*, 3985–3999.

(16) Chin, D., and Means, A. R. (2000) Calmodulin: a prototypical calcium sensor. *Trends Cell Biol. 10*, 322–328.

(17) Bahler, M., and Rhoads, A. (2002) Calmodulin signaling via the IQ motif. *FEBS Lett. 513*, 107–113.

(18) Houdusse, A., Gaucher, J. F., Krementsova, E., Mui, S., Trybus, K. M., and Cohen, C. (2006) Crystal structure of apo-calmodulin bound to the first two IQ motifs of myosin V reveals essential recognition features. *Proc. Natl. Acad. Sci. U. S. A. 103*, 19326–19331.

(19) Spudich, J. A. (2001) The myosin swinging cross-bridge model. *Nat. Rev. Mol. Cell Biol. 2*, 387–392.

(20) Kohler, D., Struchholz, S., and Bahler, M. (2005) The two IQ-motifs and Ca^{2+}/calmodulin regulate the rat myosin 1d ATPase activity. *FEBS J. 272*, 2189–2197.

(21) Barylko, B., Binns, D. D., and Albanesi, J. P. (2000) Regulation of the enzymatic and motor activities of myosin I. *Biochim. Biophys. Acta 1496*, 23–35.

(22) De La Roche, M. A., Lee, S. F., and Cote, G. P. (2003) The *Dictyostelium* class I myosin, MyoD, contains a novel light chain that lacks high-affinity calcium binding sites. *Biochem. J. 374*, 697–705.

(23) Crawley, S. W., De La Roche, M. A., Lee, S. F., Li, Z., Chitayat, S., Smith, S. P., and Cote, G. P. (2006) Identification and characterization of an 8-kDa light chain associated with *Dictyostelium discoideum* MyoB, a class I myosin. *J. Biol. Chem. 281*, 6307–6315.

(24) Levi, S., Polyakov, M., and Egelhoff, T. T. (2000) Green fluorescent protein and epitope tag fusion vectors for *Dictyostelium discoideum*. *Plasmid 44*, 231–238.

(25) Ulbricht, B., and Soldati, T. (1999) Production of reagents and optimization of methods for studying calmodulin-binding proteins. *Protein Expr. Purif. 15*, 24–33.

(26) Pang, K. M., Lynes, M. A., and Knecht, D. A. (1999) Variables controlling the expression level of exogenous genes in *Dictyostelium*. *Plasmid 41*, 187–197.

(27) Sussman, M. (1987) Cultivation and synchronous morphogenesis of Dictyostelium under controlled experimental conditions. *Methods Cell Biol. 28*, 9–29.

(28) Manstein, D. J., and Hunt, D. M. (1995) Overexpression of myosin motor domains in *Dictyostelium*: Screening of transformants and purification of the affinity tagged protein. *J. Muscle Res. Cell Motil. 16*, 325–332.

(29) Perkins, D. N., Pappin, D. J., Creasy, D. M., and Cottrell, J. S. (1999) Probability-based protein identification by searching sequence databases using mass spectrometry data. *Electrophoresis 20*, 3551–3567.

(30) Lee, S.-F., and Côté, G. P. (1995) Purification and characterization of a *Dictyostelium* protein kinase required for the actin-activated MgATPase activity of *Dictyostelium* myosin ID. *J. Biol. Chem. 270*, 11776–11782.

(31) Sreerama, N., and Woody, R. W. (2000) Estimation of protein secondary structure from circular dichroism spectra: comparison of CONTIN, SELCON, and CDSSTR methods with an expanded reference set. *Anal. Biochem. 287*, 252–260.

(32) Schuck, P. (2000) Size-distribution analysis of macromolecules by sedimentation velocity ultracentrifugation and lamm equation modeling. *Biophys. J. 78*, 1606–1619.

(33) Eswar, N., Eramian, D., Webb, B., Shen, M. Y., and Sali, A. (2008) Protein structure modeling with MODELLER. *Methods Mol. Biol. 426*, 145–159.

(34) Laskowski, R. A., Rullmannn, J. A., MacArthur, M. W., Kaptein, R., and Thornton, J. M. (1996) AQUA and PROCHECK-NMR: programs for checking the quality of protein structures solved by NMR. *J. Biomol. NMR 8*, 477–486.

(35) Wiederstein, M., and Sippl, M. J. (2007) ProSA-web: interactive web service for the recognition of errors in three-dimensional structures of proteins. *Nucleic Acids Res. 35*, W407–W410.

(36) Rosel, D., Puta, F., Blahuskova, A., Smykal, P., and Folk, P. (2000) Molecular characterization of a calmodulin-like *Dictyostelium* protein CalB. *FEBS Lett. 473*, 323–327.

(37) Burgess, W. H., Jemiolo, D. K., and Kretsinger, R. H. (1980) Interaction of calcium and calmodulin in the presence of sodium dodecyl sulfate. *Biochim. Biophys. Acta 623*, 257–270.

(38) Novak, K. D., and Titus, M. A. (1998) The myosin I SH3 domain and TEDS rule phosphorylation site are required for in vivo function. *Mol. Biol. Cell 9*, 75–88.

(39) Pollard, T. D., and Korn, E. D. (1973) *Acanthamoeba* myosin. I. Isolation from *Acanthamoeba castellanii* of an enzyme similar to muscle myosin. *J. Biol. Chem. 248*, 4682–4690.

(40) Lee, S.-F., and Côté, G. P. (1993) Isolation and characterization of three Dictyostelium myosin-I isozymes. *J. Biol. Chem. 268*, 20923–20929.

(41) Zhu, T., Sata, M., and Ikebe, M. (1996) Functional expression of mammalian myosin Iβ: Analysis of its motor activity. *Biochemistry 35*, 513–522.

(42) Collins, K., Sellers, J. R., and Matsudaira, P. (1990) Calmodulin dissociation regulates brush border myosin I (110-kD-calmodulin) mechanochemical activity in vitro. *J. Cell Biol. 110*, 1137–1147.

(43) Toya, M., Motegi, F., Nakano, K., Mabuchi, I., and Yamamoto, M. (2001) Identification and functional analysis of the gene for type I myosin in fission yeast. *Genes Cells 6*, 187–199.

(44) Lieto-Trivedi, A., and Coluccio, L. M. (2008) Calcium, nucleotide, and actin affect the interaction of mammalian Myo1c with its light chain calmodulin. *Biochemistry 47*, 10218–10226.

(45) Gillespie, P. G., and Cyr, J. L. (2002) Calmodulin binding to recombinant myosin-1c and myosin-1c IQ peptides. *BMC Biochem. 3*, 31.

(46) Lin, T., Tang, N., and Ostap, E. M. (2005) Biochemical and motile properties of Myo1b splice isoforms. *J. Biol. Chem. 280*, 41562–41567.

(47) Grotsch, H., Giblin, J. P., Idrissi, F. Z., Fernandez-Golbano, I. M., Collette, J. R., Newpher, T. M., Robles, V., Lemmon, S. K., and Geli, M. I. (2010) Calmodulin dissociation regulates Myo5 recruitment and function at endocytic sites. *EMBO J. 29*, 2899–2914.

(48) Stoffler, H. E., and Bahler, M. (1998) The ATPase activity of Myr3, a rat myosin I, is allosterically inhibited by its own tail domain and by Ca^{2+} binding to its light chain calmodulin. *J. Biol. Chem. 273*, 14605–14611.

(49) Martin, S. R., and Bayley, P. M. (2004) Calmodulin bridging of IQ motifs in myosin-V. *FEBS Lett. 567*, 166–170.

(50) Martin, S. R., and Bayley, P. M. (2002) Regulatory implications of a novel mode of interaction of calmodulin with a double IQ-motif target sequence from murine dilute myosin V. *Protein Sci. 11*, 2909–2923.

(51) Black, D. J., Tran, Q. K., and Persechini, A. (2004) Monitoring the total available calmodulin concentration in intact cells over the physiological range in free Ca^{2+}. *Cell Calcium 35*, 415–425.

(52) Liu, T., Williams, J. G., and Clarke, M. (1992) Inducible expression of calmodulin antisense RNA in Dictyostelium cells inhibits the completion of cytokinesis. *Mol. Biol. Cell 3*, 1403–1413.

(53) Grabarek, Z. (2006) Structural basis for diversity of the EF-hand calcium-binding proteins. *J. Mol. Biol. 359*, 509–525.